Curcumenol mitigates chondrocyte inflammation by inhibiting the NF-κB and MAPK pathways, and ameliorates DMM-induced OA in mice

XIAO YANG[*], YIFAN ZHOU[*], ZHIQIAN CHEN, CHEN CHEN, CHEN HAN, XUNLIN LI, HAIJUN TIAN, XIAOFEI CHENG, KAI ZHANG, TANGJUN ZHOU and JIE ZHAO

Shanghai Key Laboratory of Orthopedic Implants, Department of Orthopedics, Ninth People's Hospital, Shanghai Jiaotong University School of Medicine, Shanghai 200011, P.R. China

Abstract. At present, an increasing number of individuals are affected by osteoarthritis (OA), resulting in a heavy socioeconomic burden. OA in knee joints is caused by the release of inflammatory cytokines and subsequent biomechanical and structural deterioration. To determine its anti-inflammatory function, the current study investigated the use of the plant-derived medicine, curcumenol, in OA treatment. Curcumenol was not cytotoxic to ATDC5 chondrocytes and primary chondrocytes, as determined using a cell viability test. When these cells were treated with TNF-α and IL-1β to induce inflammation, curcumenol treatment inhibited the progression of inflammation by inactivating the NF-κB and MAPK signaling pathways, as well as decreasing the expression levels of MMP3 (as indicated by reverse transcription-quantitative PCR and western blotting). Moreover, to analyze metabolic and catabolic status in high-density and pellet culture, catalytic changes and the degradation of the extracellular matrix induced by TNF-α and IL-1β, were evaluated by alcian blue staining. These catalytic deteriorations were ameliorated by curcumenol. Using curcumenol in disease management, the mechanical and metabolic disruption of cartilage caused in the destabilization of medial meniscus (DMM) model was prevented *in vivo*. Thus, curcumenol mitigated inflammation in ATDC5 chondrocytes and primary mice chondrocytes, and also ameliorated OA in a DMM-induced mouse model.

Introduction

Osteoarthritis (OA) is a degenerative joint disorder causing disability in the elderly population worldwide (1), and is estimated to potentially affect ~400 million individuals in China by 2030 (2). OA has caused a heavy socioeconomic burden, which costs almost 2.5% of the gross domestic product of developed countries (3). Generally speaking, joints (especially the knee joint) are flexible, act as a functional motif to withstand compressive forces, and allow for a multi-directional range of motion for movement. Joints are composed of articular cartilage, subchondral bone and synovium, which are all severely compromised by OA, but especially the cartilage. However, the etiology of OA is complicated, particularly that which is associated with anatomic hip dysplasia or joint morphology (4), or that caused by immune factors, including rheumatoid arthritis (5). Thus, the management of OA is currently focused on pain relief and functional reconstruction. These conventional strategies include oral non-steroidal anti-inflammatory drugs (6), intra-articular injection of glucocorticoids (2) or hyaluronic acid (7), and surgical methods such as arthroscopic management and total arthroplasty. Stem cell injection therapy has gained significant attention in basal research and clinical trials (8); however, based on challenges such as cell leakage, osteogenic transformation of mesenchymal stem cells and other safety concerns, long-term complications and the cost-effectiveness of the procedure should be addressed (9,10). Therefore, from the prospective of the underlying molecular mechanism of OA progression, inhibiting inflammatory pathways, such as the NF-κB or MAPK cascades, may help to alleviate the progression of joint degeneration.

Curcumenol is a bioactive ingredient isolated from edible rhizome of *Curcuma zedoaria* (zedoary, Zingiberaceae), which is an important constituent of Chinese Traditional Medicine (11,12). Subsequently, curcumenol was found to be one of the primary constituents in numerous other plants, such as various Piper species, *Torilis japonica* and *Neolitsea pallens* (13,14). Such plants exhibit various functions,

Correspondence to: Dr Jie Zhao or Dr Tangjun Zhou, Shanghai Key Laboratory of Orthopedic Implants, Department of Orthopedics, Ninth People's Hospital, Shanghai Jiaotong University School of Medicine, 639 Zhizaoju Road, Shanghai 200011, P.R. China
E-mail: profzhaojie@126.com
E-mail: zhoutangjun@outlook.com

[*]Contributed equally

including anti-inflammatory, hepatoprotective, neuroprotective and antioxidant activities (15,16). Thus, curcumenol may be considered a potential option for treating inflammation.

The aim of the present study was to investigate the potential use of curcumenol to treat OA *in vitro* and *in vivo*. First, the inhibitory effect of curcumenol on the NF-κB and MAPK pathways was determined in ATDC5 chondrocytes and primary chondrocytes *in vitro*, after which the rescue function of curcumenol in destabilization of medial meniscus (DMM)-induced knee joint OA in mice was evaluated *in vivo*.

Materials and methods

Reagents. Curcumenol was purchased from Selleck Chemicals, and according to the manufacturer's protocol, was isolated from *Curcuma zedoary*, with the following characteristics: High performance liquid chromatography, purity=99.89%; nuclear magnetic resonance, consistent structure. Then, 10 mg curcumenol was dissolved in 0.4268 ml DMSO (Sigma-Aldrich; Merck KGaA) to a concentration of 100 mM, and stored at -20°C. Recombinant TNF-α (PeproTech China) and IL-1β (R&D Systems, Inc.) were dissolved in sterile PBS containing 0.1% BSA (Beyotime Institute of Biotechnology) to a concentration of 10 μg/ml.

Primary antibodies against IKKα (cat. no. D3W6N; rabbit monoclonal), phosphorylated (p)-IKKα/β (Ser176/180; cat. no. 16A6; rabbit monoclonal), P65 (cat. no. D14E12; rabbit monoclonal), p-P65 (Ser536; cat. no. 93H1; rabbit monoclonal), IκBα (cat. no. L35A5; mouse monoclonal), p-IκBα (Ser32; cat. no. 14D4; rabbit monoclonal), Akt (cat. no. 11E7; rabbit monoclonal), p-Akt (Ser473; cat. no. D9E; rabbit monoclonal), SAPK/JNK (cat. no. 9252; rabbit monoclonal), p-SAPK/JNK (Thr183/Tyr185, G9; cat. no. 81E11; rabbit monoclonal), P38 (cat. no. D13E1; rabbit monoclonal), p-P38 (Thr180/Tyr182; cat. no. D13.14.4E; rabbit monoclonal), p44/42 (cat. no. 137F5; rabbit monoclonal), p-p44/42 (Thr202/Tyr204; cat. no. D3F9; rabbit monoclonal) and β-actin (cat. no. D6A8; rabbit monoclonal) were purchased from Cell Signaling Technology, Inc. Primary antibodies against collagen type II α 1 chain (Col2a1; cat. no. ab188570; rabbit monoclonal), MMP3 (cat. no. ab52915; rabbit monoclonal), MMP7 (cat. no. ab5706; rabbit monoclonal) and MMP13 (cat. no. ab51072; rabbit monoclonal) were obtained from Abcam.

Isolation and culture of primary mouse chondrocytes. For each isolation process, three 5-day-old mice (weight, 2-4 g; Shanghai Lab, Animal Research Center Co., Ltd.; housed under pathogen-free conditions at 26-28°C and 50-65% humidity with a 12-h day/night cycle.) were sacrificed via decapitation and immersed in 75% ethanol for 10 min. Both of the lower limbs were dissected, and the skin removed, and the whole knee joint was extracted with the synovial and muscle tissue stripped. These six cartilage samples were cut into pieces (0.5-1 mm) and then soaked in 1% collagenase II solution for 2 h at 37°C, followed by centrifugation (in 300 x g, 37°C for 5 min) and resuspension in complete medium (DMEM/F12 with 5% FBS, 1% penicillin-streptomycin). The primary chondrocytes were cultured in DMEM/F12 (Gibco; Thermo Fisher Scientific, Inc.) supplemented with 5% FBS, 1% penicillin-streptomycin (Gibco; Thermo Fisher Scientific,

Inc.) and 1% insulin-transferrin-selenium (ITS) solution at 37°C with 5% CO_2.

ATDC5 cell culture. Mouse ATDC5 immortalized chondrocytes (17) were purchased from Shaanxi Fuheng (FH) Biotechnology Co., Ltd., and were maintained in DMEM/F12 supplemented with 5% FBS and 1% penicillin-streptomycin (Gibco; Thermo Fisher Scientific, Inc.) at 37°C with 5% CO_2.

RNA extraction and reverse transcription-quantitative PCR (qPCR). ATDC5 and primary chondrocytes were stimulated with TNF-α and IL-1β (both 10 ng/ml) with or without curcumenol (50 μM), and the control group was cultured in medium with 1:2,000 DMSO. After 24 h at 37°C, total RNA was isolated from cells using TRIzol® reagent (Thermo Fisher Scientific, Inc.) according to the manufacturer's protocol. Extracted RNA was reverse transcribed to first strand cDNA using the cDNA Synthesis kit (Takara Bio, Inc.). qPCR was conducted using the TB Green Premix Ex Taq kit (Takara Bio, Inc.) on an Applied Biosystems QuantStudio 6 Flex Real-Time PCR system (Applied Biosystems; Thermo Fisher Scientific, Inc.) per the following conditions: Denaturation at 95°C for 30 sec; 40 cycles of 95°C for 3 sec and 60°C for 34 sec; and then 95°C for 15 sec, 60°C for 60 sec and finally, 95°C for 15 sec. Primers were designed using NCBI BLAST (18), the sequences of which are provided in Table I. Target gene expression levels were determined using the $2^{-\Delta\Delta Cq}$ method (19), with GAPDH as the internal reference control.

Cell viability analysis. Cell viability was evaluated using the Cell Counting Kit-8 (CCK-8; Dojindo Molecular Laboratories, Inc.). ATDC5 chondrocytes were seeded into a 96-well plate at a density of 3×10^3 cells/well. The next day, the cells were treated with increasing concentrations of curcumenol (12.5, 25, 50 and 100 μM, dissolved in DMSO) for 24, 48 and 72 h at 37°C; the control group was cultured in medium containing 1:1,000 DMSO. Media were refreshed every 2 days. Subsequently, the cells were incubated with fresh complete media containing 10 μl CCK-8 reagent, for 2 h at 37°C. Complete medium containing CCK-8 reagent, with no cells or untreated cells, were used as the blank and mock controls, respectively. Absorbance at 450 nm (mean optical density; OD) was measured using an Infinite M200 Pro multimode microplate reader (Tecan Group, Ltd.).

High-density culture and pellet culture. To assess chondrogenic differentiation, 1.5×10^5 ATDC5 or primary chondrocytes were resuspended in 10 μl incomplete MEM/F12 (Gibco; Thermo Fisher Scientific, Inc.) and seeded as micromasses in the bottom of a 24-well plate. The cells were allowed to adhere for 1 h at 37°C, after which 0.5 ml MEM/F12 containing 10 ng/ml ITS and 2% FBS were added. After 24 h at 37°C, the cells were stimulated with TNF-α and IL-1β (both 10 ng/ml) with or without curcumenol (50 μM), and the control groups were cultured in a medium with DMSO only (1:2,000) for 9 days at 37°C. All media were refreshed every other day, and after 9 days the micromasses were stained with alcian blue for 24 h at room temperature (RT).

For pellet culture, 1.5×10^7 ATDC5 were pelleted in 15-ml centrifuge tubes (200 x g, 37°C for 5 min) supplemented with

Table I. PCR primer information.

Gene	Accession number	Description	Sequence (5'-3')
MMP3	NM_010809.2	Forward	CCCTGCAACCGTGAAGAAGA
		Reverse	GACAGCATCCACCCTTGAGT
MMP7	NM_010810.5	Forward	CCCTGTTCTGCTTTGTGTGTC
		Reverse	AGGGGGAGAGTTTTCCAGTCA
MMP13	NM_008607.2	Forward	AGAAGTGTGACCCAGCCCTA
		Reverse	GGTCACGGGATGGATGTTCA
ADAMTS4	NM_172845.3	Forward	GAGTCCCATTTCCCGCAGA
		Reverse	GCAGGTAGCGCTTTAACCCT
ADAMTS5	NM_011782.2	Forward	GAGAACCCTGCAAAACAGCC
		Reverse	AACCATACAAGTGCCTTTTCTCT
Col2a1	NM_053593.2	Forward	GTGTGACACTGGGAATGTCCTCT
		Reverse	TGGCCCTAATTTTCCACTGGC
GAPDH	NM_008084.3	Forward	CGACTTCAACAGCAACTCCCACTCTTCC
		Reverse	TGGGTGGTCCAGGGTTTCTTACTCCTT

ADAMTS, ADAM metallopeptidase with thrombospondin type 1 motif.

mesenchymal stem cell chondrogenic differentiation medium (Cyagen Biosciences, Inc.). After 48 h at 37˚C, the ATDC5 and primary chondrocyte pellets were stimulated with TNF-α and IL-1β (both 10 ng/ml) with or without curcumenol (50 µM), and the control group was cultured in medium containing DMSO only (1:2,000) for 21 days at 37˚C. The media were refreshed every 3 days. After 21 days of culture, the pellets were collected and fixed at RT in 4% paraformaldehyde (PFA) for 5 h, and then embedded in optimal cutting temperature compound (Sakura Finetek USA, Inc.). The samples were then stored at -80˚C overnight and cut to a 20-µm thickness using a freezing microtome (Leica Microsystems GmbH).

Digital images were captured under a light microscope at a x7.8 magnification (Leica DM4000 B; Leica Microsystems GmbH). Alcian blue staining intensity was analyzed using Image Pro Plus 6.0 software (20) to evaluate the ratio of integrated (I)OD (expressed as the IOD/area for each sample).

Senescence assays. The senescence of primary chondrocytes was analyzed using the Senescence β-Galactosidase Staining kit (Beyotime Institute of Biotechnology). Primary chondrocytes were seeded into a 12-well plate at a density of $4x10^5$ cells/well, following stimulation with TNF-α and IL-1β (10 ng/ml each) with or without curcumenol (50 µM). After 24 h at 37˚C, the cells were fixed with Beyotime Fixative Solution for 15 min at room temperature, and then incubated with Beyotime β-Galactosidase Staining buffer at 37˚C overnight. Digital images were captured under a light microscope at x10x and x20 magnification (Leica DM4000 B; Leica Microsystems GmbH) and the percentage of positive cells was calculated.

Western blot analysis. ATDC5 and primary chondrocytes were stimulated with TNF-α and IL-1β (10 ng/ml each) with or without curcumenol (50 µM). After 24 h at 37˚C, total cellular proteins were extracted for detection of MMP family and Col2a1 protein expression. For preventive analysis of the NF-κB and MAPK pathways, ATDC5 and primary chondrocytes were pretreated with increasing concentrations of curcumenol (6.25, 12.5, 25 and 50 µM, dissolved in DMSO) for 2 h at 37˚C, and then stimulated with TNF-α and IL-1β for 10 min at 37˚C, then total cellular proteins were extracted. For reactive analysis of the NF-κB and MAPK pathways, ATDC5 chondrocytes were pretreated with serum-free medium for 2 h at 37˚C and then stimulated with TNF-α with or without curcumenol for 10 min at 37˚C; total cellular proteins were then extracted.

Cultured cells were lysed using RIPA lysis buffer supplemented with phosphatase and protease inhibitors (Roche Diagnostics). The protein was quantified by BCA assay (Thermo Fisher Scientific, Inc.) and then equal quantities of extracted protein (20-30 µg) were separated via 10 or 12.5% SDS-PAGE and electroblotted onto 0.22-µm PVDF membranes (MilliporeSigma). The membranes were blocked with 5% BSA-PBS (Beyotime Institute of Biotechnology) at room temperature for 1 h, and then incubated with primary antibodies against IKKα, phosphorylated (p)-IKKα/β, P65, p-P65, IκBα, p-IκBα, Akt, p-Akt, SAPK/JNK, p-SAPK/JNK, P38, p-P38, p44/42, p-p44/42 and β-actin overnight (≥16 h) at 4˚C. The membranes were washed with TBS-0.1% Tween20 (TBST) and subsequently incubated with anti-rabbit IgG (H+L) secondary antibody (cat. no. 5151; DyLight™ 800 4X PEG Conjugate; Cell Signaling Technology, Inc.; 1:5,000) for 1 h at room temperature in the dark. After washing in TBST, protein immunoreactivity was detected using the Odyssey Fluorescence Imaging system (LI-COR Biosciences). Semi-quantitative analysis of protein band intensity was conducted using ImageJ V1.8.0 software (National Institutes of Health) and normalized to the internal loading control, β-actin.

Animals and surgical procedures. All animal experiments were approved by the Institutional Animal Care and Ethics

Committee of Ninth People's Hospital, Shanghai Jiaotong University School of Medicine (Shanghai, China), and performed in accordance with the principles and procedures of the National Institutes of Health Guide for the Care and Use of Laboratory Animals, and the Guidelines for Animal Treatment of Shanghai Jiaotong University. A total of 18 8-week-old male C57/BL mice (weight, 18-22 g; Shanghai Lab, Animal Research Center Co., Ltd.) were housed under pathogen-free conditions at 26-28°C and 50-65% humidity with a 12-h day/night cycle. Animals were fed standard rodent chow and had access to fresh water *ad libitum*. Before the surgical procedures, mice were anesthetized by intraperitoneal injection of pentobarbital sodium (50 mg/kg of body weight). In the control group (n=6; underwent sham surgery and were treated with corn oil; however, during research, one mouse was lost from the control group), the fur on the skin was shaved, a 0.5-cm incision was made near the right knee joint, and the ligamentum patellae was exposed and stretched. The remaining 12 mice were assigned to the DMM group (n=6; underwent DMM surgery and were treated with corn oil; 1 mouse was removed from the DMM group to equalize the numbers) and the curcumenol group (n=6; underwent DMM surgery and were treated with curcumenol; one was removed from curcumenol group to equalize the numbers). After exposure, the medial collateral ligaments were transected, and the medial meniscus of the tibia was partially removed using a 5-mm blade micro-surgical knife (Beyotime Institute of Biotechnology) (21). After the operation, the incisions were sutured and the mice were initially treated two days after surgery, and then for another 2 months with intraperitoneal injections of curcumenol (50 mg curcumenol pre-dissolved in 1 ml DMSO and then diluted in 100 ml corn oil) for the curcumenol group, and corn oil (cat. no. C8267; Sigma-Aldrich; Merck KGaA; 1 ml DMSO diluted in 100 ml corn oil) for the control and DMM groups, at 4 mg/kg/time twice a week. At the end of the experimental period, all mice were sacrificed by cervical dislocation and the right lower limbs were extracted, cleaned of soft tissues, stretched and fixed in 4% PFA at RT for 48 h.

Histology and immunofluorescence staining. Fixed lower limb samples were embedded in paraffin and subjected to histological sectioning (5-μm thickness). For histological assessment, paraffin-embedded tissue sections were processed for Safranin O-Fast Green and hematoxylin and eosin (H&E) staining (Servicebio) at RT for 2-5 min, in accordance with the manufacturer's instructions. Sections were examined for tissue thickness, which was quantified by measuring the Safranin O-positive thickness in the center of the medial tibial plateau (22,23), and the OA Research Society Internationall histological (OARSI) score system: 0, normal; 0.5, loss of Safranin-O without structural changes; 1, small fibrillations without loss of cartilage; 2, vertical clefts down to the layer immediately below the superficial layer and some loss of surface lamina; 3, vertical clefts/erosion to the calcified cartilage extending to <25% of the articular surface; 4, vertical clefts/erosion to the calcified cartilage extending to 25-50% of the articular surface; 5, vertical clefts/erosion to the calcified cartilage extending to 50-75% of the articular surface; and 6, vertical clefts/erosion to the calcified cartilage extending >75% of the articular surface.

For immunofluorescence assessment, ATDC5 cells were cultured on slides added to a 6-well plate. At 10% confluence, the cells were stimulated with TNF-α and IL-1β for 20 min at 37°C, with or without curcumenol pretreatment for 2 h at 37°C. Then the slides were fixed with 4% PFA at RT for 48 h, and then immersed in PBS (pH 7.4) and washed three times for 5 min each. Auto-fluorescence quencher was added to the sections for 5 min, which were then blocked with blocking buffer (Cell Signaling Technology, Inc.) for 30 min at RT. The slides were subsequently incubated with primary antibodies in a wet box at 4°C overnight. Anti-pp65 primary antibody was used at a 1:100 dilution. The following day, the slides were washed with PBS and incubated with N Alexa Fluor 594-conjugated secondary antibody (cat. no. 8889; anti-rabbit; 1:500; Cell Signaling Technology, Inc.) for 50 min at RT in the dark. Subsequently, the slides were washed with PBS and then incubated with DAPI solution (Sigma-Aldrich; Merck KGaA) for 10 min at RT in the dark to stain cell nuclei. After a final wash with PBS, the samples were air-dried and sealed with anti-fluorescence quenching tablets. Digital fluorescence images were captured under a Leica DM4000 B epifluorescence microscope (Leica Microsystems GmbH) at a x10 and x20 magnification, and IOD measurements were obtained using Image Pro Plus 6.0 software (Media Cybernetics, Inc.).

For tissue staining, the sections were de-paraffinized in graded xylene, rehydrated in graded alcohol solutions, and then incubated in antigen retrieval buffer (Roche Diagnostics) at 37°C for 30 min. After cooling to RT, the sections were immersed in PBS (pH 7.4) and washed three times for 5 min each, and then processed as slides as aforementioned. Anti-TNF-α (cat. no. ab183218; Abcam), anti-IL-1β (cat. no. ab234437; Abcam) and anti-Col2a1 (cat. no. AF0135; Affinity) primary antibodies were used at a 1:100 dilution.

Immunohistochemistry. Fixed lower limb samples were embedded in paraffin as aforementioned, and cut into slices (8 μm), then subjected to immunohistochemistry using a kit (cat. no. G1215-200T; Wuhan Servicebio Technology Co., Ltd.) according to the manufacturer's instructions. Briefly, tissue sections were incubated with rabbit anti-TNF-α (cat. no. ab9579; Abcam), anti-IL-1β (cat. no. ab283818; Abcam) and anti-Col2a1 (cat. no. ab34712; Abcam) overnight at 4°C (1:100 dilution). The following day, the slides were washed with PBS and incubated with goat anti-mouse/rabbit IgG HRP-polymer (cat. no. 91196; anti-rabbit; 1:500; Cell Signaling Technology, Inc.) for 30 min at RT using 3,3'-diaminobenzidin as the chromogen. Digital images were captured under a Leica DM4000 B microscope at x10 and x20 magnification, and positively-stained cell measurements were obtained using Image Pro Plus 6.0 software.

Radiographic analysis. Digital X-ray imaging of the right lower limbs was conducted per the manufacturer's instructions (24) in the anteroposterior axis with a 21 lp/mm detector that provides up to x5 geometric magnification (Faxitron VersaVision; Faxitron Bioptics LLC).

Statistical analysis. A total of three independent experiments or repeated measurements were conducted for all data. Data are presented as the mean ± SD. Differences between study groups were analyzed by one-way ANOVA with Tukey's post
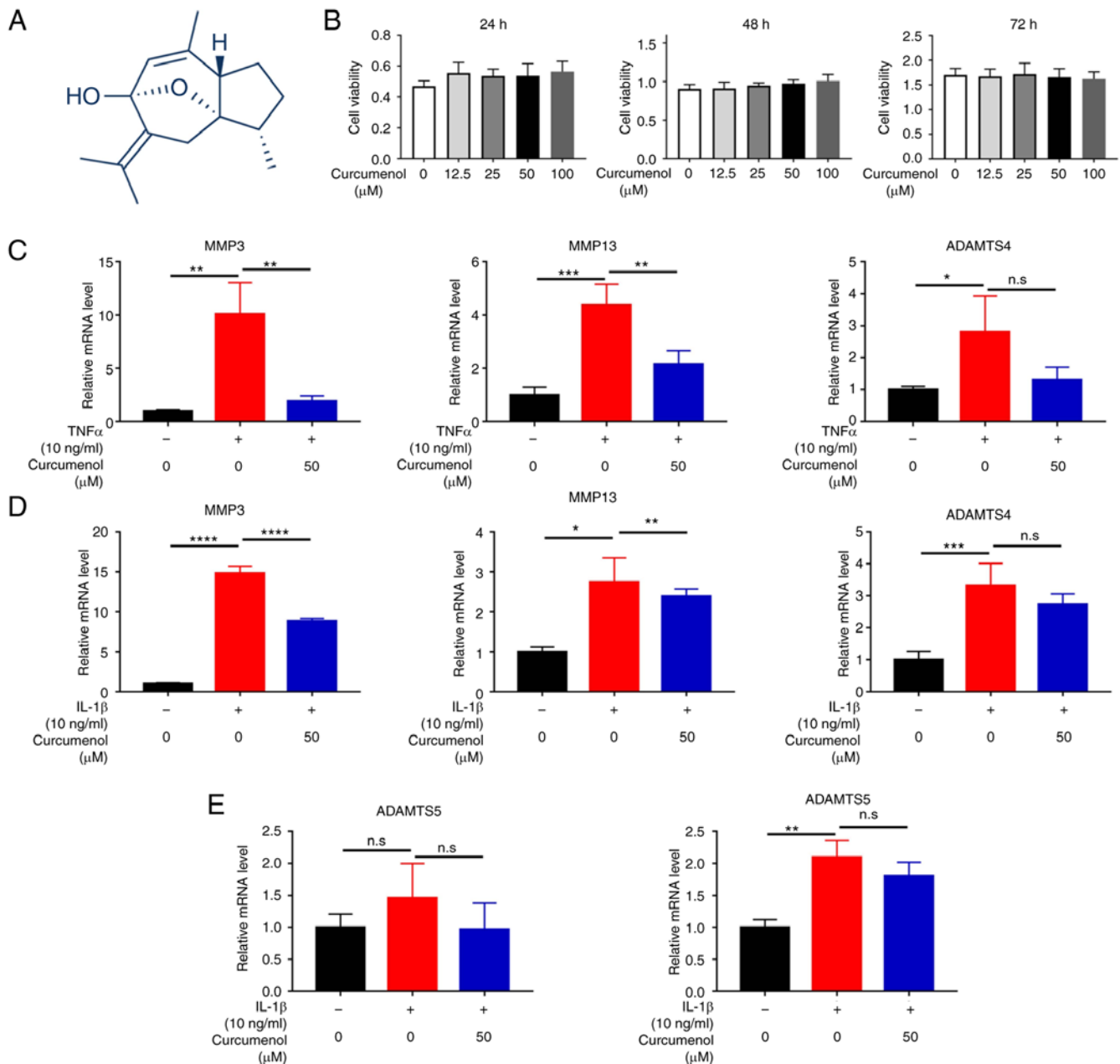
Figure 1. Curcumenol is not cytotoxic to ATDC5 chondrocytes, and inhibits TNF-α and IL-1β–induced MMP family upregulation *in vitro*. (A) Chemical structure of curcumenol. (B) Cell Counting Kit-8 assay results of ATDC5 chondrocytes stimulated with curcumenol at different concentrations (0, 12.5, 25, 50 and 100 μM) and over different time periods (24-72 h). (C) RT-qPCR analysis of relative mRNA expression levels of MMP3, MMP13 and ADAMTS4 in ATDC5 chondrocytes with TNF-α (10 ng/ml) or/and curcumenol (50 μM) administration. (D) RT-qPCR analysis of relative mRNA expression levels of MMP3, MMP13 and ADAMTS4 in ATDC5 chondrocytes with IL-1β (10 ng/ml) or/and curcumenol (50 μM) administration for 24 h. (E) RT-qPCR analysis of relative mRNA expression levels of ADAMTS5 in ATDC5 chondrocytes with TNF-α (10 ng/ml) and IL-1β (10 ng/ml) with or without curcumenol (50 μM) administration. All data are presented as the mean ± SD from three experiments. $^*P<0.05$, $^{**}P<0.01$, $^{***}P<0.001$ and $^{****}P<0.0001$. RT-qPCR, reverse transcription-quantitative PCR; ADAMTS4, ADAM metallopeptidase with thrombospondin type 1 motif 4; ADAMTS5, ADAM metallopeptidase with thrombospondin type 1 motif 5.

hoc test. Significant differences in ordinal data between study groups were assessed by Kruskal-Wallis test with a Dunn's post hoc test. Analyses were conducted using SPSS 19.0 software (IBM Corp.), and P<0.05 was considered to indicate a statistically significant difference.

Results

Curcumenol inhibits MMP family upregulation induced by TNF-α and IL-1β in ATDC5 chondrocytes. Curcumenol is a bioactive ingredient isolated from *Curcuma zedoaria*, and

its chemical structure is shown in Fig. 1A. Considering its safety for the treatment of OA, CCK-8 assays were conducted to evaluate curcumenol cytotoxicity in ATDC5 chondrocytes. Concentrations of 12.5, 25, 50 and 100 μM curcumenol were not cytotoxic towards ATDC5 chondrocytes, and did not affect the proliferation rate of these cells between 24 and 72 h (Fig. 1B); 50 μM was selected for further experimentation, as in our preliminary studies, RT-qPCR and western blotting revealed that the effects of 100 μM curcumenol were not considerably different to those after 50 μM treatment (data not shown). To further investigate the anti-inflammatory

effects of curcumenol on ATDC5 chondrocytes, TNF-α and IL-1β (10 ng/ml, 24 h) were used to activate the inflammatory response. The expression of the MMP3, MMP13, ADAM metallopeptidase with thrombospondin type 1 motif 4 (ADAMTS4) and ADAMTS5 genes was increased following TNF-α (Fig. 1C and E) and IL-1β (Fig. 1D and E) stimulation. However, following treatment with 50 μM curcumenol, the expression levels of these genes were significantly decreased; ADAMTS gene expression was also downregulated, but not to a significant degree (Fig. 1C-E). Western blotting was conducted to determine the effects of curcumenol on protein expression levels in ATDC5 chondrocytes. After stimulation with TNF-α and IL-1β, MMP3 expression was increased, and 50 μM curcumenol effectively mitigated the upregulation of MMP3 protein (Figs. S1E-H). Moreover, Col2a1 expression decreased following inflammation induction, and was subsequently increased by curcumenol treatment, though not significantly so. In conclusion, curcumenol safely and effectively inhibited the TNF-α- and IL-1β-induced upregulation of MMP family proteins in ATDC5 chondrocytes.

Curcumenol mitigates TNF-α and IL-1β induced inflammation in ATDC5 cells by inhibiting the phosphorylation of NF-κB and MAPK pathway components. To further investigate the underlying mechanisms by which curcumenol inhibits inflammation, ATDC5 cells were treated with various curcumenol concentrations following stimulation with TNF-α and IL-1β. For NF-κB pathway analysis, the levels of p-IKKα, p-P65 and p-IκBα were significantly increased 10 min after TNF-α and IL-1β stimulation (Fig. 2A and E). Although curcumenol had little effect on p-IKKα, it effectively decreased the upregulation of p-P65 and p-IκBα. Moreover, curcumenol increased the total inflammation-induced protein expression level of IκBα (Fig. 2A and E). The quantification analysis revealed a significant rescue effect of curcumenol on p-P65 and p-IκBα, following both TNF-α (Fig. 2B-D) and IL-1β (Fig. 2F-H) stimulation.

For MAPK pathway analysis (10 min is the only timepoint used in this study), curcumenol effectively inhibited the phosphorylation of SAPK/JNK, but showed a minimal inhibitory effect on ERK and P38 phosphorylation in a short time period (Figs. S1A and S1C). Quantification also revealed a significant rescue effect of curcumenol on p-SAPK/JNK, but not on p-ERK/ERK and p-p38/p38 (Fig. S1B and S1D). Based on immunofluorescence analysis, after stimulation with TNF-α and IL-1β, P65 was phosphorylated and translocated into the cell nucleus within 20 min, but curcumenol treatment was able to effectively block the phosphorylation and translocation of P65 (Fig. 3A and B). The results indicated that in ATDC5 chondrocytes, curcumenol exerted an inhibitory effect on NF-κB and MAPK pathway activation induced by TNF-α and IL-1β.

Curcumenol modifies TNF-α and IL-1β-induced catabolic status in high-density culture and pellet culture. The dynamic status between catabolism and metabolism was analyzed using alcian blue staining of high-density and pellet cultures. ATDC5 chondrocytes were cultured at high-density culture, and TNF-α and IL-1β stimulation was found to disrupt the extracellular matrix (ECM) of the micromass (Fig. 3C and E). However, the damage to the ECM was significantly reversed by curcumenol treatment (Fig. 3D and F).

In pellet culture, the ATDC5 pellets of the control group showed abundant ECM, while in the TNF-α and IL-1β groups, the pellets were shrunken and the ECM was degraded, with decreased Safranine O staining. Moreover, curcumenol was able to rescue this disruption, recovering the ECM to near normal status (Fig. S2A and C), with the ratio of Safranin O-Fast Green decreased in the TNF-α and IL-1β group, and increased in the curcumenol group (Fig. S2B and D). Therefore, curcumenol effectively altered catabolism status following deterioration by inflammatory cytokines, and partially rescued micromass and pellet damage.

Curcumenol exerts an anti-inflammatory effect on primary chondrocytes by inhibiting the NF-κB and MAPK pathway in vitro. Considering the prospect of using curcumenol in clinical practice, the current study aimed to isolate mouse primary chondrocytes to further confirm the anti-inflammatory function of curcumenol (Fig. 4A). Curcumenol effectively mitigated the ECM degradation induced by TNF-α and IL-1β (Fig. 4D-G). Moreover, the TNF-α- and IL-1β-induced senescence of primary chondrocytes was rescued by curcumenol treatment (Fig. S3A-D). Following stimulation with inflammatory cytokines, the number of cells stained with β-gal (blue stain) increased, suggesting that these cells aged under stress; however, with curcumenol treatment number of aging cells decreased compared with the TNF-α or IL-1β group. The results demonstrated that TNF-α stimulation activated the classical inflammation (NF-κB and MAPK) pathways, and immediately increased the phosphorylation of IKKα, P65, IκBα, Akt, SAPK/JNK, P44/P42 and P38. However, after pre-treatment with curcumenol, the phosphorylation of P65, IκBα and SAPK/JNK was significantly inhibited (Fig. S3E and F). Furthermore, the degradation of IκBα was rescued by curcumenol treatment (Fig. S3E). After these pathways were inhibited with curcumenol, the catabolic MMP family genes were similarly downregulated compared with the inflammation-induced cells alone (Fig. 4H), as shown by the reduced expression of MMP3, MMP7 and MMP13 (Fig. 4B and C), which further confirmed the current hypothesis. With regards to the chondrogenic marker Col2a1, curcumenol significantly rescued its downregulation following inflammatory stimulation (Fig. 4B, C and H). Based on the aforementioned results, curcumenol was not only functional in ATDC5 cells, but also exerted anti-inflammatory effects in primary chondrocytes.

Curcumenol alleviates DMM-induced OA in mice by inhibiting TNF-α expression. In addition to its preventative effects *in vitro*, curcumenol also significantly inhibited the phosphorylation of P65, IκBα and SAPK/JNK (Fig. S4A and B). Thus, to further investigate the possibility of clinical curcumenol use, a DMM-induced OA model was established in mice, and intraperitoneally-injected curcumenol was used to mitigate this degeneration (the exact number of mice in every group was 6; however, during the research, 1 mouse was lost from the control group, and 1 was removed from each of the other two groups to equalize the numbers). As presented in Fig. 5A, DMM-induced OA was severe, with additional osteophyte formation and the collapse of the joint space. As shown by the H&E and Safranine O-Fast green staining, curcumenol
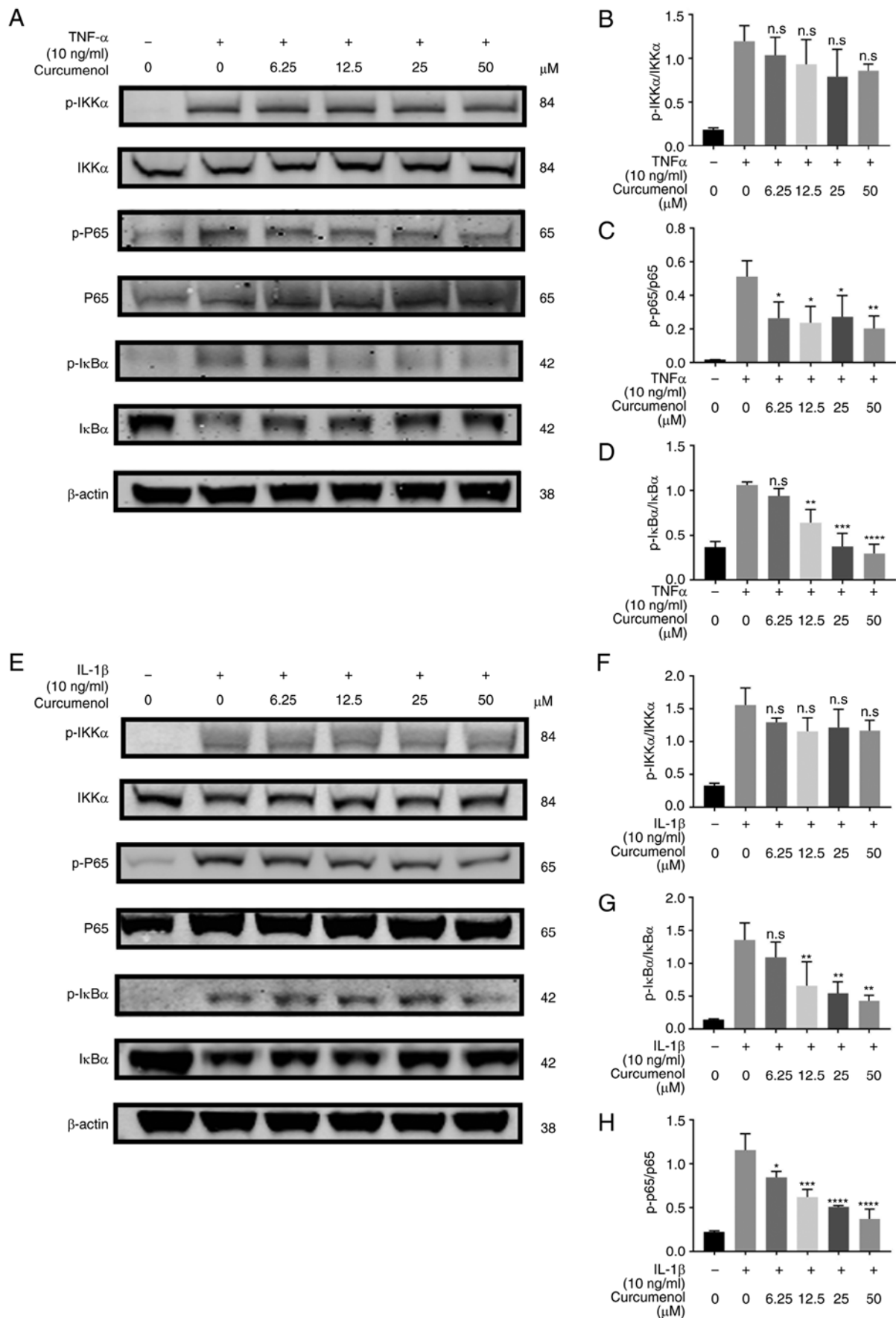
Figure 2. Curcumenol inhibits TNF-α and IL-1β-induced phosphorylation of NF-κB pathway in ATDC5 cells. (A-D) Western blot analysis of p-IKKα, IKKα, p-P65, P65, p-IκBα and IκBα expression in ATDC5 chondrocytes stimulated with TNF-α (10 ng/ml) for 10 min (E-H) Western blot analysis of p-IKKα, IKKα, p-P65, P65, p-IκBα and IκBα expression in ATDC5 chondrocytes stimulated with IL-1β (10 ng/ml) for 10 min. Cells were pretreated with 0, 6.25, 12.5, 25 and 50 μM curcumenol. Grey scale values were generated using β-actin as the internal reference. All data are presented as mean ± SD from three experiments. *P<0.05, **P<0.01, ***P<0.001 and ****P<0.0001. p-, phosphorylated.
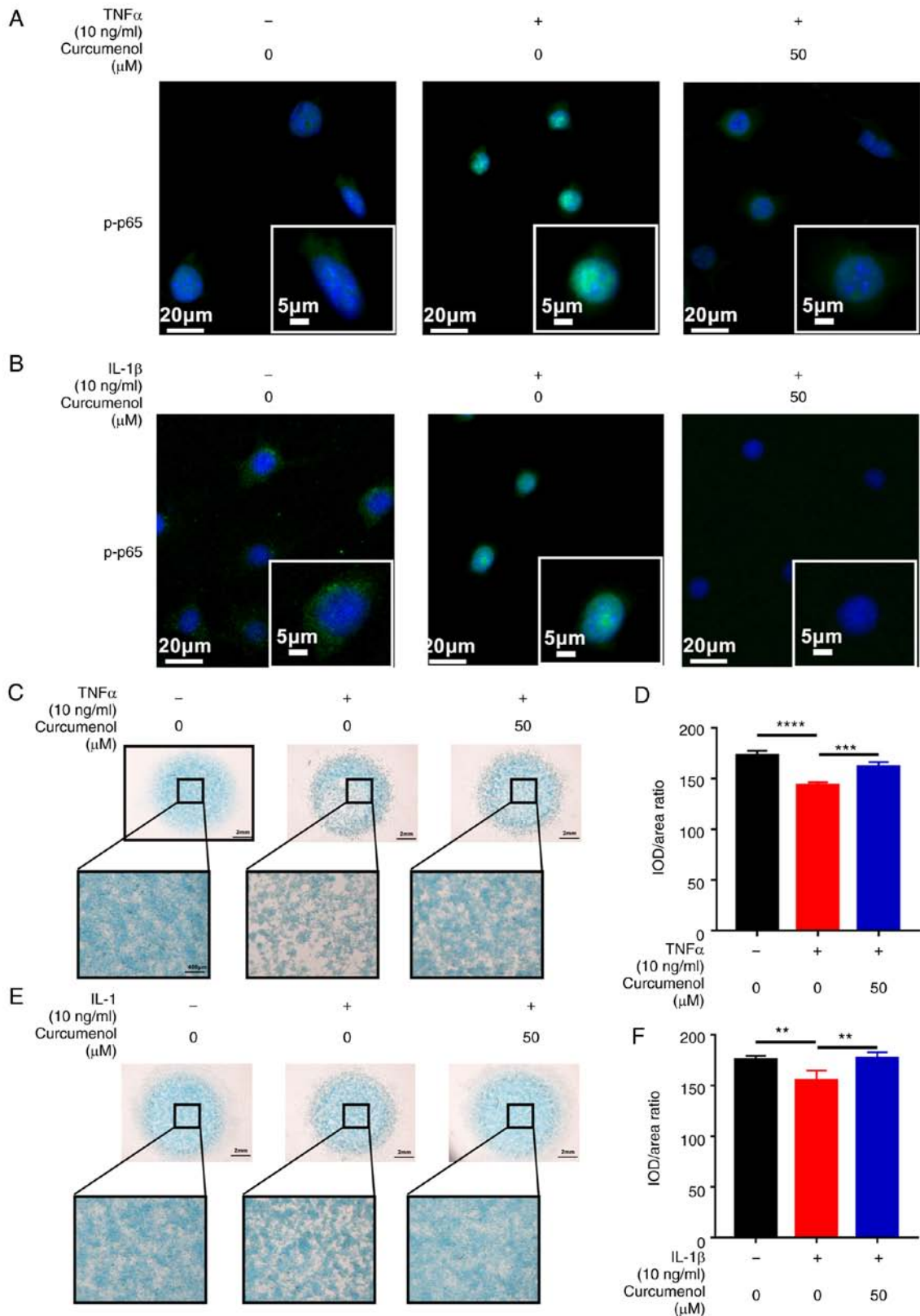
Figure 3. Curcumenol modifies catabolism status induced by TNF-α and IL-1β in high-density culture. Immunofluorescence analysis for phosphorylation and translocation of P65 in ATDC5 chondrocytes pretreated with 50 μM curcumenol and stimulated with (A) TNF-α (10 ng/ml) or (B) IL-1β (10 ng/ml) for 20 min. (C and D) Alcian blue staining of ATDC5 chondrocytes using high-density culture, stimulated with TNF-α (10 ng/ml) or/and curcumenol (50 μM) for 9 days. (E and F) Alcian blue staining of ATDC5 chondrocytes using high-density culture stimulated with IL-1β (10 ng/ml) or/and curcumenol (50 μM) for 9 days. Ratio of IOD/area was analyzed using Image Pro Plus 6.0. All data are presented as mean ± SD from three experiments. $^{**}P<0.01$ and $^{***}P<0.001$ and $^{****}P<0.0001$. Col2a1, collagen type II α 1 chain; IOD, integrated optical density.

prevented further degeneration of the cartilage surrounding the tibia and femur (Fig. 5B). Cartilage tissue thickness was also significantly restored (Fig. 5E), and the OARIS histological score was decreased by curcumenol compared with the DMM
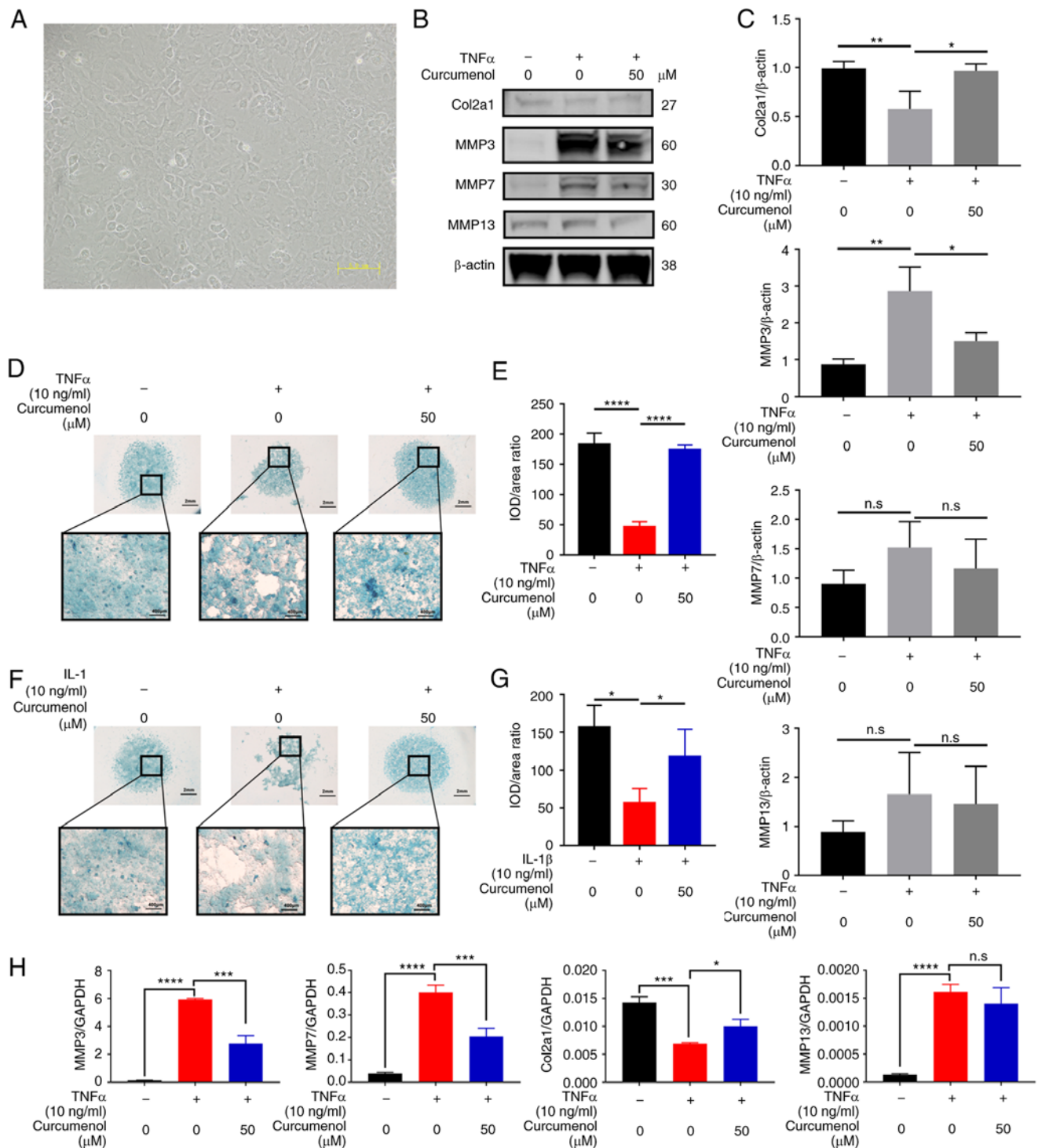
Figure 4. Curcumenol exerts an anti-inflammatory effect on primary chondrocytes by inhibiting MMP family protein expression, rescuing high-density culture *in vitro*. (A) Successful isolation of primary chondrocytes from mice. (B and C) Western blot analysis of Col2a1, MMP3, MMP7 and MMP13 expression in primary chondrocytes stimulated with TNF-α (10 ng/ml) or/and 50 μM curcumenol for 24 h. Grey scale values were generated using β-actin as the internal reference. (D and E) Alcian blue staining of primary chondrocytes using high-density culture stimulated with TNF-α (10 ng/ml) or/and curcumenol (50 μM) for 9 days. (F and G) Alcian blue staining of primary chondrocytes using high-density culture stimulated with IL-1β (10 ng/ml) or/and curcumenol (50 μM) for 9 days. Ratio of IOD/area was analyzed using Image Pro Plus 6.0. (H) Reverse transcription-quantitative PCR analysis of the relative mRNA expression levels of MMP3, MMP7, MMP13 and Col2a1 in primary chondrocytes with TNF-α (10 ng/ml) or/and curcumenol (50 μM) treatment for 24 h. All data are presented as mean ± SD from three experiments. *$P<0.05$, **$P<0.01$, ***$P<0.001$ and ****$P<0.0001$. Col2a1, collagen type II α 1 chain; IOD, integrated optical density.

group (Fig. 5D). The immunohistochemistry results demonstrated that TNF-α and IL-1β expression was activated in the DMM group, but that the levels of these inflammatory cytokines were decreased by curcumenol treatment. By contrast, Col2a1 was decreased in the DMM group, but was recovered by curcumenol treatment (Fig. 5C and G). In line with the immunohistochemistry results, immunofluorescence revealed an increase in TNFα and IL-1β, and a decrease in Col2a1 in the DMM group, which were decreased by curcumenol treatment (Fig. 5F and H). Collectively, the results indicated that
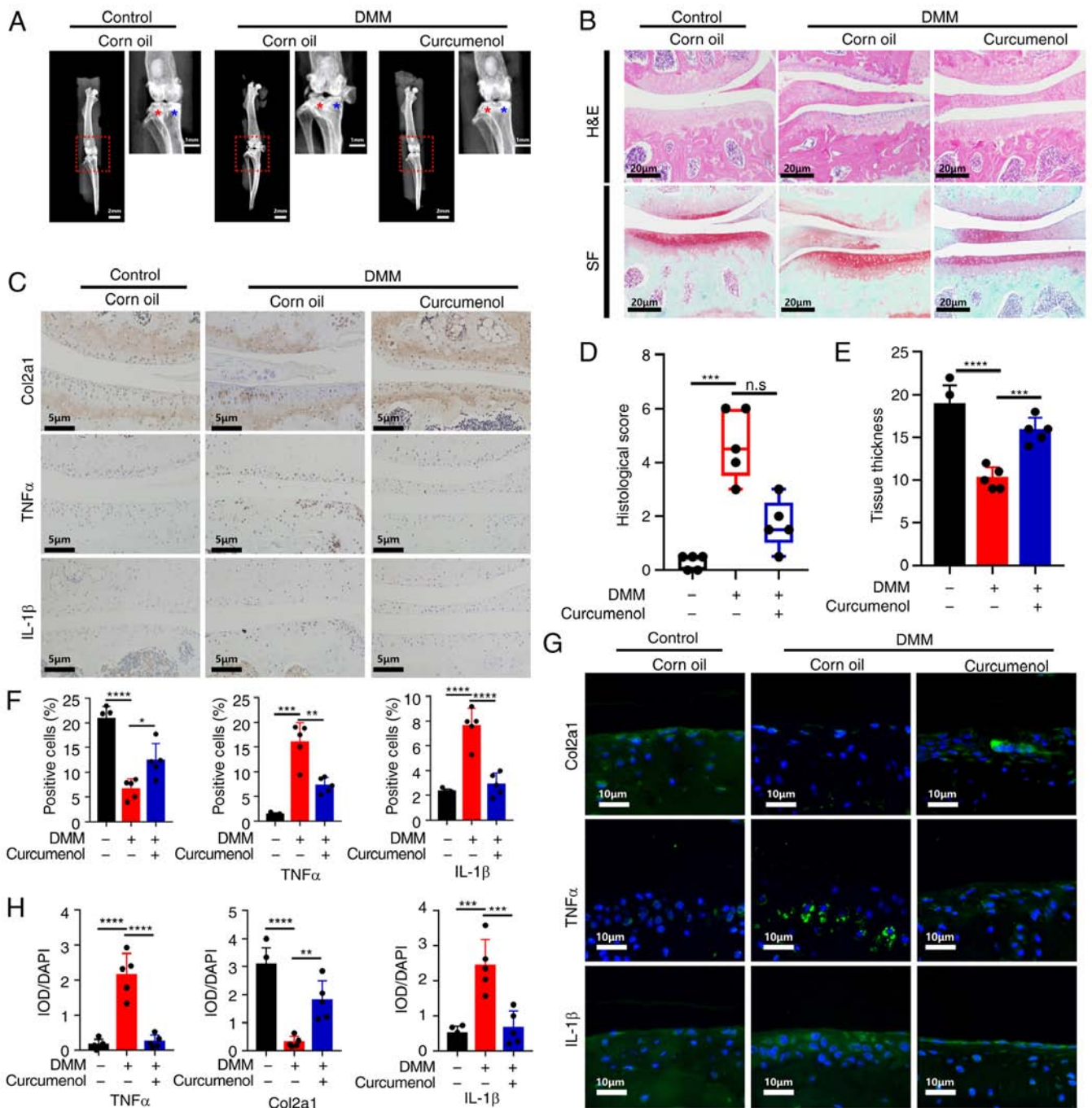
Figure 5. Curcumenol treats DMM-induced osteoarthritis in mice by inhibiting TNF-α and IL-1β *in vivo*. (A) X-ray of lower limbs. (B) Safranin O-Fast Green and hematoxylin & eosin staining of paraffin sections of the medial chondrocyte end plate of knee joints at a coronal position. (C) Immunohistochemical analysis of Col2a1, TNF-α and IL-1β expression in knee joints at a coronal position. (D and E) Quantification of histological score and tissue thickness in the sections described in (B). (F) Quantification of positive cells in sections described in (C). (G and H) Immunofluorescence analysis of Col2a1, TNF-α and IL-1β expression in knee joints at a coronal position. Data are presented as mean ± SD using one-way ANOVA with a Tukey's post hoc test; ordinal data were analyzed by Kruskal-Wallis test and Dunn's post hoc test from three experiments. $^{*}P<0.05$, $^{**}P<0.01$, $^{***}P<0.001$ and $^{****}P<0.0001$. Col2a1, collagen type II α 1 chain; IOD, integrated optical density; DMM, destabilization of medial meniscus.

curcumenol exerted an inhibitory effect on inflammatory cascades such as the NF-κB and MAPK pathways *in vitro*, and was involved in the rescue of DMM-induced osteoarthritis *in vivo*.

Discussion

OA, associated with age-related degeneration, immune reactivity and trauma, affects an increasing number of individuals worldwide, and leads to suboptimal health status and disability (25). At present, the primary treatment for OA is surgical intervention, which aims to achieve symptomatic relief, and while this treatment is effective as an end-stage choice, it can also be traumatic and with numerous side-effects (26). Thus, OA lacks early and mid-term treatment options to ameliorate and cure this chronic disease.

Non-steroidal anti-inflammatory drugs, and some analgesics, are the conventional medicines used to manage
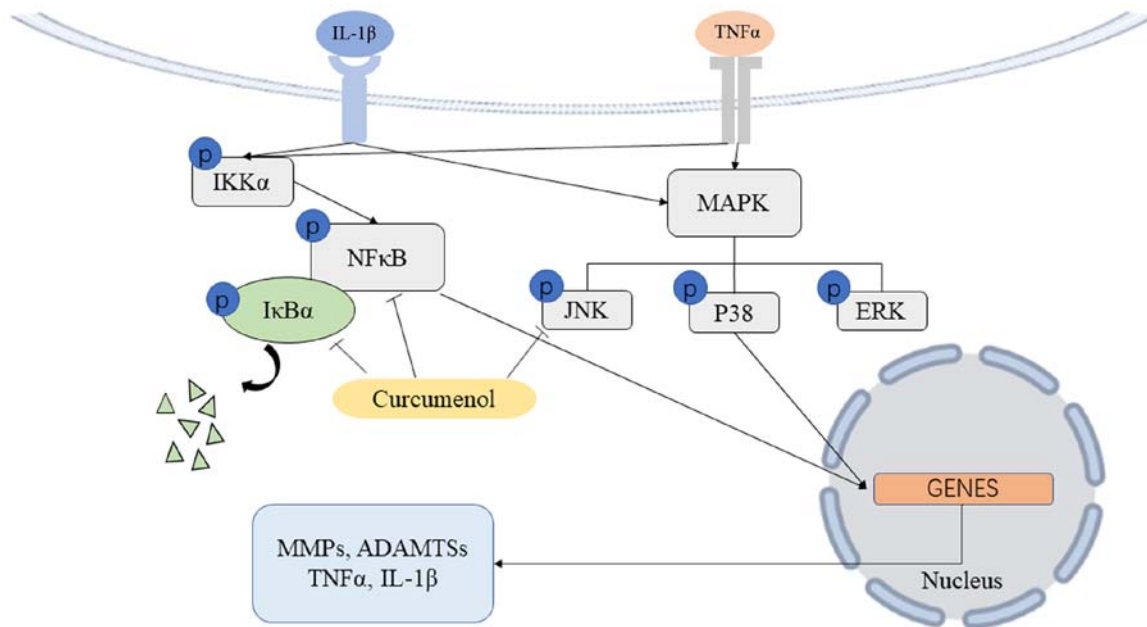
Figure 6. Curcumenol inhibits the phosphorylation and activation of the NF-κB and MAPK pathways induced by TNF-α and IL-1β, and prevents inflammatory cascade reactions in chondrocytes *in vitro*. Moreover, curcumenol serves as a protector in destabilization of medial meniscus-induced osteoarthritis model mice by inhibiting TNF-α- and IL-1β-activated inflammation *in vivo*. ADAMTS, ADAM metallopeptidase with thrombospondin type 1 motif.

OA (27,28), but the side-effects of these drugs, such as hepatic damage and gastrointestinal injury, are concerns for their long-term usage (29). Due their reduced side-effects, abundant production capacities and anti-inflammatory functions, plant-derived traditional medicines have gained increasing attention in previous years (30-32). Therefore, the present study investigated whether traditional medicines could be used to ameliorate the symptoms and slow the progression of OA.

Curcumenol is a bioactive compound isolated from edible rhizome of *Curcuma zedoaria*, with potential anti-inflammatory effects (33). Curcumenol belongs to the *Curcuma* genus, and one of the most well-known members is *Curcuma longa*, of which the bioactive extraction curcumin is used to treat synovitis experienced by patients with knee OA (34). Considering the broad application range of the *Curcuma* genus, and the role of proinflammatory cytokines such as TNF-α and IL-1β in the pathophysiology of OA (35), the current study aimed to investigate the anti-inflammatory effects of curcumenol to treat TNF-α- and IL-1β-induced inflammation in ATDC5 and primary chondrocytes. The present results also demonstrated that curcumenol ameliorated the effects of OA in the knee joints of DMM-model mice *in vivo*.

DMM surgery was used to generate a mechanical OA model. During joint degeneration, especially that of the cartilage, the levels of some inflammatory cytokines, (including TNF-α and IL-1β) are increased, and subsequently cause a progressive, cell-mediated cascade of molecular and structural deterioration (36,37). TNF-α and IL-1β exert their detrimental functions via multiple important intracellular cascades, such as the NF-κB and MAPK pathways (38,39), In general, TNF-α and IL-1β transmit inflammatory signals via their receptors and activate the phosphorylation of the IKK complex (40), which then phosphorylates IκBα (41). Subsequently, IκBα is unbound and phosphorylates NF-κB, which translocates into the nucleus to initiate the transcription

of inflammatory products, catabolic enzymes and apoptotic mediators (42-45). Curcumenol blocks the phosphorylation and translocation of NF-κB, and inhibits the phosphorylation of IκBα, to block the anti-inflammatory function. With regards to the MAPK pathway, curcumenol prevents the phosphorylation of JNK, which belongs to a large family of serine/threonine kinases and crosslinks with numerous developmental pathways, such as Hippo signaling (46), promoting proteoglycan metabolism and inhibiting the production of catabolic enzymes and inflammatory mediators in chondrocytes (47) and the nucleus pulposus (48). After TNF-α stimulation, the expression levels of MMPs are increased and the production of ECM is inhibited, which promotes the ECM to change to a catabolic and degradable status (49,50). This imbalance causes the senescence of primary chondrocytes, followed by instability and cartilage loss in joints (51). In the present study, curcumenol was used to successfully inhibit the phosphorylation of IκBα, NF-κB P65 subunit and SAPK/JNK (Fig. 6). At the same time, the nuclear translocation of p-P65 was blocked, which lead to a subsequent decrease in MMP expression and the rescue of type 2 collagen in ATDC5 and primary chondrocytes. Thus, it was suggested that inhibiting the function of these cytokines may be beneficial in the DMM-induced OA model.

The DMM-induced OA model in mice is an effective animal model first established in 2007 (21), whereby removing the medial meniscus can pathologically disrupt the stability status of normal knee joints, which can restrict the range of motion (52). Using the widely recognized DMM-induced model, the present study demonstrated the rescue effect of curcumenol in OA of the knee joint, as it effectively mitigated inflammation in the cartilage of the tibia and femur, as well as preventing joint space collapse and osteophyte formation. The mechanism underlying this damage was consistent with the *in vitro* data. The immunohistochemistry results revealed

an increase in TNF-α and IL-1β expression in the DMM group, which triggered the subsequent detrimental molecular cascade and degeneration. In the curcumenol-treated group, TNF-α and IL-1β expression was downregulated and Col2a1 expression was restored, demonstrating the curative effect of curcumenol in DMM-induced OA *in vivo*. Another important consideration is how to reconstitute and administer curcumenol, as it is insoluble in water. Therefore, DMSO was used in the present study to pre-dissolve curcumenol, which was then diluted in non-pharmaceutical grade corn oil, which showed little adverse effect during intraperitoneal injection in mice (53,54). With regard to the administration method, intraperitoneal injection was selected rather than intraarticular administration, based on the following: i) Intraperitoneal injection of corn oil is widely used in mouse models and the only administration method of curcumenol in mice appears to be intraperitoneal injection (55); and ii) there is a possibility of cartilage injury (56,57) and difficulties associated with injecting corn oil via multiple micro-injections into the knee joint.

The current study confirmed the efficiency and safety of curcumenol, but there are still some concerns and limitations to our studies. For efficiency, the systemic distribution of curcumenol after intraperitoneal injection was not assessed, thus there was a lack of direct evidence that the optimal concentration of curcumenol reached the joint. In subsequent studies, the concentration of curcumenol in in the blood will first be assessed, and then preliminary investigations of curcumenol distribution in the knee joint tissues will be conducted. For safety, although the intraperitoneal injection of curcumenol is relatively safe with corn oil (53), treatment-induced injury was not evaluated. In subsequent studies, relevant experiments will be conducted, such as the evaluation of paraffin sections of lung, liver, heart, kidney and spleen, to further confirm the safety of curcumenol *in vivo*. Furthermore, the administration method was via intraperitoneal injection, which in clinical use, may be more difficult when treating patients. Therefore, the efficiency and safety of oral administration in DMM-induced osteoarthritis or type II collagen (UC-II) diminished deterioration of articular cartilage will be investigated in mice (58,59).

In conclusion, the current study presented a novel plant-derived bioactive medicine, curcumenol, which was demonstrated to serve as a potential anti-inflammatory agent for the management of OA. The low cytotoxicity, reduced side-effects and high production capacity are also considerable advantages of future curcumenol use in the clinic.

Acknowledgements

Availability of data and materials

The datasets used and/or analyzed during the current study are available from the corresponding author on reasonable request.

Authors' contributions

JZ and TZ guided the study, making substantial contributions to conception and design. XY and YZ performed the experiments. XY, YZ, CH and XL interpreted the data and drafted the manuscript. KZ, ZC and CC performed the statistical analysis and reviewed the manuscript critically for important intellectual content. HT and XC confirmed the authenticity of all the raw data. All authors read and approved the final manuscript.

Ethics approval and informed consent

Animal Ethics approval was received from the Institutional Animal Ethics Review Board of Shanghai Ninth People's Hospital, Shanghai Jiao Tong University School of Medicine (approval no. SH9H-2020-A559-1). Written informed consent was obtained from all participants.

Patient consent for publication

Not applicable.

Competing interests

The authors declare that they have no competing interests.

References

1. Glyn-Jones S, Palmer AJ, Agricola R, Price AJ, Vincent TL, Weinans H and Carr AJ: Osteoarthritis. Lancet 386: 376-387, 2015.
2. Zhang Z, Huang C, Jiang Q, Zheng Y, Liu Y, Liu S, Chen Y, Mei Y, Ding C, Chen M, *et al*: Guidelines for the diagnosis and treatment of osteoarthritis in China (2019 edition). Ann Transl Med 8: 1213, 2020.
3. Hiligsmann M, Cooper C, Arden N, Boers M, Branco JC, Luisa Brandi M, Bruyère O, Guillemin F, Hochberg MC, Hunter DJ, *et al*: Health economics in the field of osteoarthritis: An expert's consensus paper from the European society for clinical and economic aspects of osteoporosis and osteoarthritis (ESCEO). Semin Arthritis Rheum 43: 303-313, 2013.
4. Agricola R, Heijboer MP, Roze RH, Reijman M, Bierma-Zeinstra SMA, Verhaar JAN, Weinans H and Waarsing JH: Pincer deformity does not lead to osteoarthritis of the hip whereas acetabular dysplasia does: Acetabular coverage and development of osteoarthritis in a nationwide prospective cohort study (CHECK). Osteoarthritis Cartilage 21: 1514-1521, 2013.
5. Tsuchiya H, Ota M, Sumitomo S, Ishigaki K, Suzuki A, Sakata T, Tsuchida Y, Inui H, Hirose J, Kochi Y, *et al*: Parsing multiomics landscape of activated synovial fibroblasts highlights drug targets linked to genetic risk of rheumatoid arthritis. Ann Rheum Dis: Nov 2, 2020 (Epub ahead of print).
6. Myers J, Wielage RC, Han B, Price K, Gahn J, Paget MA and Happich M: The efficacy of duloxetine, non-steroidal anti-inflammatory drugs, and opioids in osteoarthritis: A systematic literature review and meta-analysis. BMC Musculoskelet Disord 15: 76, 2014.
7. McAlindon TE, Bannuru RR, Sullivan MC, Arden NK, Berenbaum F, Bierma-Zeinstra SM, Hawker GA, Henrotin Y, Hunter DJ, Kawaguchi H, *et al*: OARSI guidelines for the non-surgical management of knee osteoarthritis. Osteoarthritis Cartilage 22: 363-388, 2014.

8. Pas HI, Winters M, Haisma HJ, Koenis MJ, Tol JL and Moen MH: Stem cell injections in knee osteoarthritis: A systematic review of the literature. Br J Sports Med 51: 1125-1133, 2017.
9. Hached F, Vinatier C, Le Visage C, Gondé H, Guicheux J, Grimandi G and Billon-Chabaud A: Biomaterial-assisted cell therapy in osteoarthritis: From mesenchymal stem cells to cell encapsulation. Best Pract Res Clin Rheumatol 31: 730-745, 2017.
10. Wang X, Liao T, Wan C, Yang X, Zhao J, Fu R, Yao Z, Huang Y, Shi Y, Chang G, et al: Efficient generation of human primordial germ cell-like cells from pluripotent stem cells in a methylcellulose-based 3D system at large scale. PeerJ 6: e6143, 2019.
11. Hikino H, Sakurai Y, Numabe S and Takemoto T: Structure of curcumenol. Chem Pharm Bull (Tokyo) 16: 39-42, 1968.
12. Xu J, Ji F, Kang J, Wang H, Li S, Jin DQ, Zhang Q, Sun H and Guo Y: Absolute configurations and NO inhibitory activities of terpenoids from curcuma longa. J Agric Food Chem 63: 5805-5812, 2015.
13. Assis A, Brito V, Bittencourt M, Silva L, Oliveira F and Oliveira R: Essential oils composition of four Piper species from Brazil. J Essential Oil Res 25: 203-209, 2013.
14. Saikia AK, Sarma SK, Strano T and Ruberto G: Essential oil from piper pedicellatum C. DC. Collected in North-East India. J Essential Oil Bearing Plants 18: 314-319, 2015.
15. Sun DX, Fang ZZ, Zhang YY, Cao YF, Yang L and Yin J: Inhibitory effects of curcumenol on human liver cytochrome P450 enzymes. Phytother Res 24: 1213-1216, 2010.
16. Pintatum A, Maneerat W, Logie E, Tuenter E, Sakavitsi ME, Pieters L, Berghe WV, Sripisut T, Deachathai S and Laphookhieo S: In Vitro anti-inflammatory, anti-oxidant, and cytotoxic activities of four species and the isolation of compounds from rhizome. Biomolecules 10: 799, 2020.
17. Oh CD, Im HJ, Suh J, Chee A, An H and Chen D: Rho-associated kinase inhibitor immortalizes rat nucleus pulposus and annulus fibrosus cells: Establishment of intervertebral disc cell lines with novel approaches. Spine (Plila Pa 1976) 41: E255-E261, 2016.
18. Johnson M, Zaretskaya I, Raytselis Y, Merezhuk Y, McGinnis S and Madden TL: NCBI BLAST: A better web interface. Nucleic Acids Res 36 (Web Server issue): W5-W9, 2008.
19. Livak KJ and Schmittgen TD: Analysis of relative gene expression data using real-time quantitative PCR and the 2(-Delta Delta C(T)) method. Methods 25: 402-408, 2001.
20. Shi JW, Zhang TT, Liu W, Yang J, Lin XL, Jia JS, Shen HF, Wang SC, Li J, Zhao WT, et al: Direct conversion of pig fibroblasts to chondrocyte-like cells by c-Myc. Cell Death Discov 5: 55, 2019.
21. Glasson SS, Blanchet TJ and Morris EA: The surgical destabilization of the medial meniscus (DMM) model of osteoarthritis in the 129/SvEv mouse. Osteoarthritis Cartilage 15: 1061-1069, 2007.
22. Wang M, Sampson ER, Jin H, Li J, Ke QH, Im HJ and Chen D: MMP13 is a critical target gene during the progression of osteoarthritis. Arthritis Res Ther 15: R5, 2013.
23. Loeser RF, Kelley KL, Armstrong A, Collins JA, Diekman BO and Carlson CS: Deletion of JNK enhances senescence in joint tissues and increases the severity of age-related osteoarthritis in mice. Arthritis Rheumatol 72: 1679-1688, 2020.
24. Sohara Y, Shimada H, Scadeng M, Pollack H, Yamada S, Ye W, Reynolds CP and DeClerck YA: Lytic bone lesions in human neuroblastoma xenograft involve osteoclast recruitment and are inhibited by bisphosphonate. Cancer Res 63: 3026-3031, 2003.
25. Sharma L: Osteoarthritis of the knee. N Engl J Med 384: 51-59, 2021.
26. Thorlund JB, Juhl CB, Roos EM and Lohmander LS: Arthroscopic surgery for degenerative knee: Systematic review and meta-analysis of benefits and harms. BMJ 350: h2747, 2015.
27. Rasmussen-Barr E, Held U, Grooten WJA, Roelofs PDDM, Koes BW, van Tulder MW and Wertli MM: Nonsteroidal anti-inflammatory drugs for sciatica: An updated cochrane review. Spine (Phila Pa 1976) 42: 586-594, 2017.
28. Derry S, Wiffen PJ, Kalso EA, Bell RF, Aldington D, Phillips T, Gaskell H and Moore RA: Topical analgesics for acute and chronic pain in adults-an overview of cochrane reviews. Cochrane Database Syst Rev 5: CD008609, 2017.
29. Marmon P, Owen SF and Margiotta-Casaluci L: Pharmacology-informed prediction of the risk posed to fish by mixtures of non-steroidal anti-inflammatory drugs (NSAIDs) in the environment. Environ Int 146: 106222, 2021.
30. Chen J, Xuan J, Gu YT, Shi KS, Xie JJ, Chen JX, Zheng ZM, Chen Y, Chen XB, Wu YS, et al: Celastrol reduces IL-1β induced matrix catabolism, oxidative stress and inflammation in human nucleus pulposus cells and attenuates rat intervertebral disc degeneration in vivo. Biomed Pharmacother 91: 208-219, 2017.
31. Liu Y, Deng SJ, Zhang Z, Gu Y, Xia SN, Bao XY, Cao X and Xu Y: 6-Gingerol attenuates microglia-mediated neuroinflammation and ischemic brain injuries through Akt-mTOR-STAT3 signaling pathway. Eur J Pharmacol 883: 173294, 2020.
32. Li Y, Lin S, Liu P, Huang J, Qiu J, Wen Z, Yuan J, Qiu H, Liu Y, Liu Q, et al: Carnosol suppresses RANKL-induced osteoclastogenesis and attenuates titanium particles-induced osteolysis. J Cell Physiol 236: 1950-1966, 2021.
33. Lo JY, Kamarudin MNA, Hamdi OAA, Awang K and Kadir HA: Curcumenol isolated from curcuma zedoaria suppresses Akt-mediated NF-κB activation and p38 MAPK signaling pathway in LPS-stimulated BV-2 microglial cells. Food Funct 6: 3550-3559, 2015.
34. Wang Z, Jones G, Winzenberg T, Cai G, Laslett LL, Aitken D, Hopper I, Singh A, Jones R, Fripp J, et al: Effectiveness of extract for the treatment of symptoms and effusion-synovitis of knee osteoarthritis : A randomized trial. Ann Intern Med 173: 861-869, 2020.
35. Kapoor M, Martel-Pelletier J, Lajeunesse D, Pelletier JP and Fahmi H: Role of proinflammatory cytokines in the pathophysiology of osteoarthritis. Nat Rev Rheumatol 7: 33-42, 2011.
36. Rodriguez-Trillo A, Mosquera N, Pena C, Rivas-Tobío F, Mera-Varela A, Gonzalez A and Conde C: Non-Canonical WNT5A signaling through RYK contributes to aggressive phenotype of the rheumatoid fibroblast-like synoviocytes. Front Immunol 11: 555245, 2020.
37. Zhao X, Meng F, Hu S, Yang Z, Huang H, Pang R, Wen X, Kang Y and Zhang Z: The synovium attenuates cartilage degeneration in KOA through activation of the Smad2/3-Runx1 cascade and chondrogenesis-related miRNAs. Mol Ther Nucleic Acids 22: 832-845, 2020.
38. Baker RG, Hayden MS and Ghosh S: NF-κB, inflammation, and metabolic disease. Cell Metab 13: 11-22, 2011.
39. Moqbel SAA, Xu K, Chen Z, Xu L, He Y, Wu Z, Ma C, Ran J, Wu L and Xiong Y: Tectorigenin alleviates inflammation, apoptosis, and ossification in rat tendon-derived stem cells modulating NF-Kappa B and MAPK pathways. Front Cell Dev Biol 8: 568894, 2020.
40. Zhang Q, Lenardo MJ and Baltimore D: 30 Years of NF-κB: A blossoming of relevance to human pathobiology. Cell 168: 37-57, 2017.
41. Zhongyi S, Sai Z, Chao L and Jiwei T: Effects of nuclear factor kappa B signaling pathway in human intervertebral disc degeneration. Spine (Phila Pa 1976) 40: 224-232, 2015.
42. Baldwin AS: The NF-kappa B and I kappa B proteins: New discoveries and insights. Annu Rev Immunol 14: 649-683, 1996.
43. Sun Z, Yin Z, Liu C, Liang H, Jiang M and Tian J: IL-1β promotes ADAMTS enzyme-mediated aggrecan degradation through NF-κB in human intervertebral disc. J Orthop Surg Res 10: 159, 2015.
44. Tu J, Li W, Zhang Y, Wu X, Song Y, Kang L, Liu W, Wang K, Li S, Hua W and Yang C: Simvastatin inhibits IL-1β-induced apoptosis and extracellular matrix degradation by suppressing the NF-kB and MAPK pathways in nucleus pulposus cells. Inflammation 40: 725-734, 2017.
45. Chen J, Garssen J and Redegeld F: The efficacy of bortezomib in human multiple myeloma cells is enhanced by combination with omega-3 fatty acids DHA and EPA: Timing is essential. Clin Nutr 40: 1942-1953, 2021.
46. Pham TH, Hagenbeek TJ, Lee HJ, Li J, Rose CM, Lin E, Yu M, Martin SE, Piskol R, Lacap JA, et al: Machine learning and chemico-genomics approach defines and predicts cross-talk of Hippo and MAPK pathways. Cancer Discov 11: 778-793, 2021.
47. Cao C, Wu F, Niu X, Hu X, Cheng J, Zhang Y, Li C, Duan X, Fu X, Zhang J, et al: Cadherin-11 cooperates with inflammatory factors to promote the migration and invasion of fibroblast-like synoviocytes in pigmented villonodular synovitis. Theranostics 10: 10573-10588, 2020.
48. Séguin CA, Bojarski M, Pilliar RM, Roughley PJ and Kandel RA: Differential regulation of matrix degrading enzymes in a TNFalpha-induced model of nucleus pulposus tissue degeneration. Matrix Biol 25: 409-418, 2006.
49. Wang G, Chen S, Xie Z, Shen S, Xu W, Chen W, Li X, Wu Y, Li L, Liu B, et al: TGFβ attenuates cartilage extracellular matrix degradation via enhancing FBXO6-mediated MMP14 ubiquitination. Ann Rheum Dis 79: 1111-1120, 2020.
50. He L, He T, Xing J, Zhou Q, Fan L, Liu C, Chen Y, Wu D, Tian Z, Liu B and Rong L: Bone marrow mesenchymal stem cell-derived exosomes protect cartilage damage and relieve knee osteoarthritis pain in a rat model of osteoarthritis. Stem Cell Res Ther 11: 276, 2020.

51. Inoue R, Ishibashi Y, Tsuda E, Yamamoto Y, Matsuzaka M, Takahashi I, Danjo K, Umeda T, Nakaji S and Toh S: Knee osteoarthritis, knee joint pain and aging in relation to increasing serum hyaluronan level in the Japanese population. Osteoarthritis Cartilage 19: 51-57, 2011.

52. Lamo-Espinosa JM, Blanco JF, Sánchez M, Moreno V, Granero-Moltó F, Sánchez-Guijo F, Crespo-Cullel I, Mora G, Vicente DDS, Pompei-Fernández O, *et al*: Phase II multicenter randomized controlled clinical trial on the efficacy of intra-articular injection of autologous bone marrow mesenchymal stem cells with platelet rich plasma for the treatment of knee osteoarthritis. J Transl Med 18: 356, 2020.

53. Hubbard JS, Chen PH and Boyd KL: Effects of repeated intraperitoneal injection of pharmaceutical-grade and nonpharmaceutical-grade corn oil in female C57BL/6J mice. J Am Assoc Lab Anim Sci 56: 779-785, 2017.

54. Alsina-Sanchis E, Mülfarth R, Moll I, Mogler C, Rodriguez-Vita J and Fischer A: Intraperitoneal oil application causes local inflammation with depletion of resident peritoneal macrophages. Mol Cancer Res 19: 288-300, 2021.

55. Wang S, Ma Q, Xie Z, Shen Y, Zheng B, Jiang C, Yuan P, An Q, Fan S and Jie Z: An antioxidant sesquiterpene inhibits osteoclastogenesis via blocking IPMK/TRAF6 and counteracts OVX-induced osteoporosis in mice. J Bone Miner Res: May 6, 2021 (Epub ahead of print).

56. Kompel AJ, Roemer FW, Murakami AM, Diaz LE, Crema MD and Guermazi A: Intra-articular corticosteroid injections in the hip and knee: Perhaps not as safe as we thought? Radiology 293: 656-663, 2019.

57. Mehta PN and Ghadially FN: Articular cartilage in corn oil-induced lipoarthrosis. Ann Rheum Dis 32: 75-82, 1973.

58. Bagi CM, Berryman ER, Teo S and Lane NE: Oral administration of undenatured native chicken type II collagen (UC-II) diminished deterioration of articular cartilage in a rat model of osteoarthritis (OA). Osteoarthritis Cartilage 25: 2080-2090, 2017.

59. Runhaar J, Rozendaal RM, van Middelkoop M, Bijlsma HJW, Doherty M, Dziedzic KS, Lohmander LS, McAlindon T, Zhang W and Zeinstra SB: Subgroup analyses of the effectiveness of oral glucosamine for knee and hip osteoarthritis: A systematic review and individual patient data meta-analysis from the OA trial bank. Ann Rheum Dis 76: 1862-1869, 2017.